

Chapter 15

Multipath Delay Weaken in Complex Situation

Xiang Lin, Zhiyun Han, Feng Zhou and Siyuan Guo

Abstract In order to decrease code and carrier phase error influence on distance measurement efficiently, it is used to applied multipath reduction techniques such as narrow correlator to eliminate estimation error when signal propagation in indoor space. However, these techniques depends heavily on the delayed value of autocorrelation peak. In this paper, an improved Projection Onto Convex Set algorithm (POCS) is discussed that estimate the effect the elimination of spurious noise peaks by using adaptive threshold in the Channel Impulse Response (CIR). Finally, a test was taken for pseudo-range estimation reduction in urban environment.

Keywords Projection Onto Convex Set algorithm · Adaptive threshold · Channel Impulse Response

15.1 Introduction

Accurately estimation between the locally PRN codes and the signals arriving from different satellites is much important for distance computation in global navigation satellite system. However, various signals superimposed in waveforms

X. Lin (✉) · F. Zhou · S. Guo
Beijing Satellite Navigation Center, Beijing 5128, China
e-mail: stationeffie@yahoo.cn

F. Zhou
e-mail: zhoufeng@163.com

S. Guo
e-mail: guosiyuan0714@yahoo.com.cn

Z. Han
China Space Technology Institute, Beijing, China
e-mail: stationeffie@yahoo.cn

because of the multipath effect, produce a variety of different code delay and random phase. Although much relative error of the global navigation satellite system can be calculated using the differential correction technology, the multipath phenomenon depends on the local environmental factors, not through the differential treatment. Therefore multipath effect is a much important element for pseudo-range calculation error [1].

In this paper, a improved POCS algorithm is introduced which evaluated the channel impulse using the method of adaptive threshold to remove spurious peaks in each iteration time. After calculating the channel impulse response, the arrival time of multipath signal is starting from the first signal passing threshold, whenever the signal is blocked, the first road of multipath signal arrived can be used to calculate the pseudo-range delay. Similarly, the phase shift can be calculated by correlation phase discrimination function.

15.2 Mathematical Model

The channel impulse response model in a specular multipath situation can be expressed as [2]

$$h(t) = \sum_{k=1}^N a_k \delta(t - t_k). \quad (15.1)$$

where $h(t)$ is the function of CIR, N is the number of signal paths, a_k ($a_k < 1$) is the complex attenuation factor of the k -th path. Because the received signal is the output of the multipath channel in response to the transmitted signal $s(t)$, it can be expressed as:

$$r(t) = h(t) \otimes s(t) + n(t) = \sum_{k=1}^N a_k s(t - t_k) + n(t). \quad (15.2)$$

$r(t)$ is the multipath error affected signal function, $n(t)$ is the channel additive white Gaussian noise and \otimes denotes the convolution operation.

15.3 Error Estimation

Prior to despreading, received GPS signal power is smaller than the noise. Compositing the received baseband signal into Eq. (15.2), the output signal $C(\tau)$ can be represented as followed ($b(\tau)$ means the channel impulse response):

$$C(\tau) = b(\tau) \otimes h(\tau) = \sum_{k=1}^N b(\tau - t_k)h_k + u(\tau) \quad (15.3)$$

$$b(\tau) = \frac{1}{T} \int_T s(t)s(t - \tau)dt \quad (15.4)$$

T means the code period, and $u(\tau)$ means the noise element in the output of the integration process. Equation (15.3) can be written as:

$$C = Bh + u \quad (15.5)$$

where $C = [C_1 \dots C_M]^T$ is the vector of samples of the matched filter output and B is

$$B = \begin{bmatrix} b(\tau_1 - t_1) & \cdots & b(\tau_1 - t_N) \\ \vdots & \ddots & \vdots \\ b(\tau_M - t_1) & \cdots & b(\tau_M - t_N) \end{bmatrix} \quad (15.6)$$

where $h = [h_1, \dots, h_N]$ is the true channel vector while t_1 means the true path delays. The vector u contains the samples of the complex noise in harsh environment.

15.4 Multipath Analyze

The least square method (L) is the most common method of channel vector calculation now, minimizing the square error ($\|C - Bh\|^2$) as

$$\hat{h}_L = (B^T B)^{-1} B^T C. \quad (15.7)$$

where the superscript T means a matrix transpose. \hat{h}_{\min} means the minimized squared error as ($\hat{\sigma}^2$ denotes the estimated noise variance):

$$\hat{h}_{\min} = (\hat{\sigma}^2 I + B^T B)^{-1} B^T C \quad (15.8)$$

The POCS approach is an iterative constraint-based deconvolution approach which evaluated the CIR by iterating Eq. (15.8) as [3]

$$\hat{h}_p^{(i)} = \hat{h}_p^{(i-1)} + (\hat{\sigma}^2 I + B^T B)^{-1} B^T C \left(C - B\hat{h}_p^{(i-1)} \right) \quad (15.9)$$

Here, $\hat{h}_p^{(i)}$ is the i-th estimated CIR. Equation (15.8) is used for initialization. The required number of iterations relies on the SNR level. Lower SNRs needs

larger number of iterations. Therefore, interference components of the signal is the key to solve the problem. The interference components in each signal can be applied to the related, POCS while find the relevant factors in each projection. Supposed Q is a parameter in modeling equation, then the projection onto convex sets with respect to the formula (15.10) can be expressed as:

$$\hat{h}_p = Q\{\hat{h}\} \quad (15.10)$$

If the interference factor can be effectively suppressed by computing the limited error variance or narrow value interval, Fig. 15.1 shows a diagram of the receiver implementing the POCS method. it should be noted that as the sampling rate is limited, the estimated CIR may not be ideal as Eq. (15.10). In order to perform a limited bandwidth, the estimated CIR can be expressed as follows [4]:

$$\hat{h}(t) = \sum_{k=1}^N \hat{a}(k) f_s \left[\frac{\sin(\pi(t - \hat{t}_k) f_s)}{\pi(t - \hat{t}_k) f_s} \right] \quad (15.11)$$

a_k is the complex attenuation factor of the k -th path. f is the sampling rate. Figure 15.2 show the magnitude of the estimated CIR in POCS algorithm respectively.

The LOS code delay can be used as a channel impulse response vector which reflects the maximum amplitude value. It can be expressed as:

$$\hat{\tau}_p = \arg \max_{\tau} \left| \hat{h}_p \right| \quad (15.12)$$

Here, $\hat{\tau}_p$ means the amplitude of CIR. When the LOS delay has been determined, the LOS phase offset is computed from the corresponding complex channel coefficient by applying a proper phase discriminator.

$$f = \left(\sum_{i=k/2}^{k/2} \hat{h}_p(\hat{h}_p^i)^\lambda + \frac{\sigma_n^s}{\omega} I \right) \hat{h}_p \quad (15.13)$$

where \hat{h}_p^i is \hat{h}_p shifted by i steps, K is the number of filter taps and s is a constant (Fig. 15.3).

15.5 Improved POCS

The Improved POCS algorithms with the conventional differs in the following aspects:

1. In the novel projection algorithm, author estimate the effect of CIR by adaptive threshold to eliminate the false peaks of signal. Supposed the threshold was $x\bar{z}$:

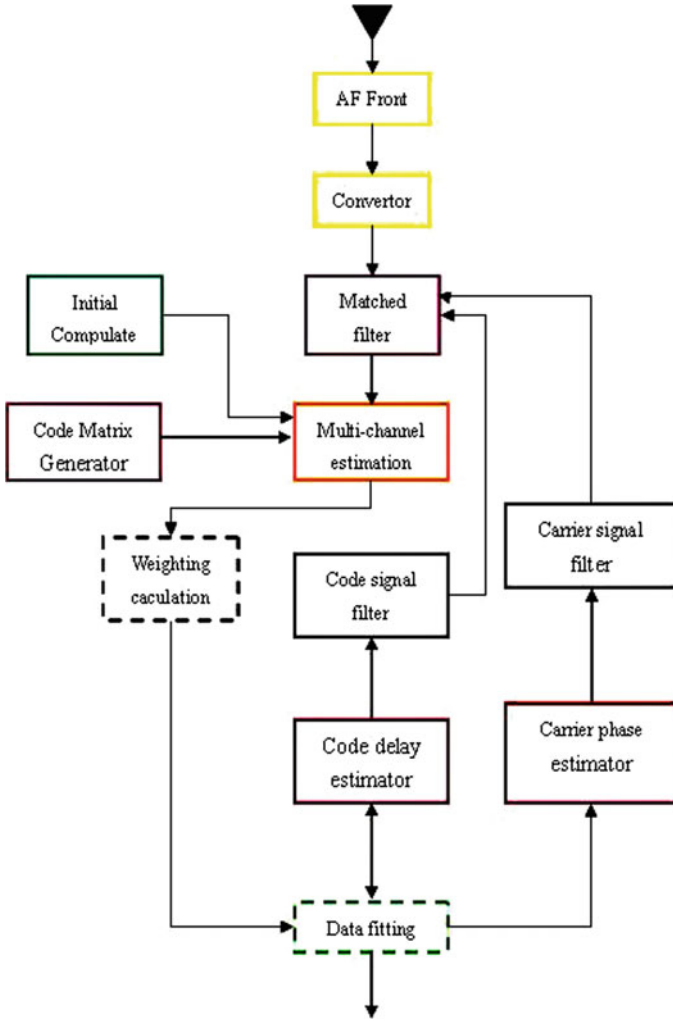


Fig. 15.1 POCS method computation diagram

$$\bar{z} = \frac{1}{N} \sum_{k=1}^N \hat{h}_P(x) / \max \{ \hat{h}_P(x) \} \tag{15.14}$$

Here, the threshold is set as $s = \min\{x_z \bar{z}, 1\}$. In all the simulations presented in this paper, x_z was set to 2.5.

2. In preview, estimation accuracy of POCS depend on the rate of signal sampling. However, the rates of signal sampling is limited in experiment. That is to say, Some real channel impulse signal is not included. In case, the larger value

Fig. 15.2 Estimated CIR magnitude in multipath environment

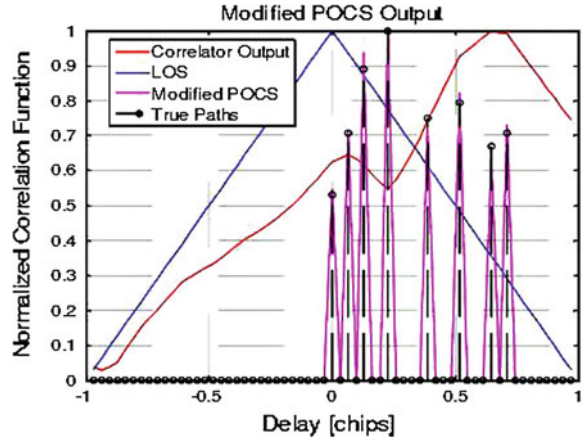
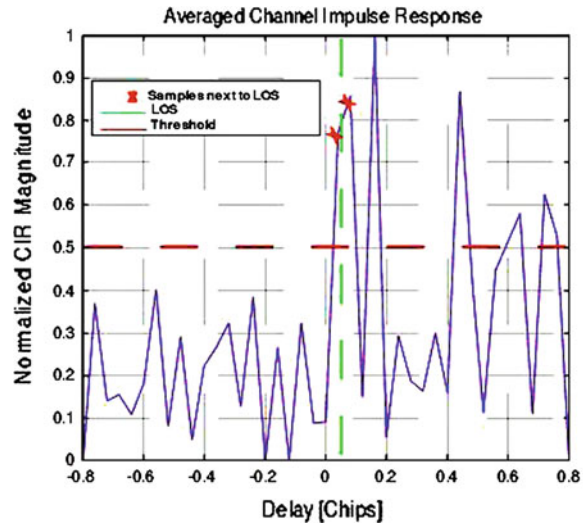


Fig. 15.3 Accuracy of TOA estimation variation tendency



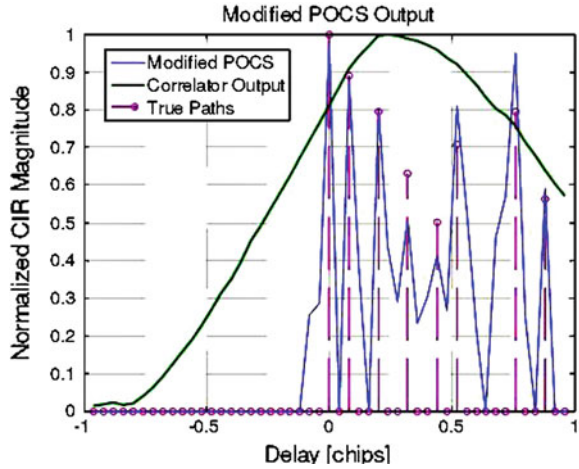
of both sides' sampling-single can be indicated the true channel component. Figure 15.4 depicts such a method.

In order to increase the accuracy of the new algorithms, we do the linear combination of sample signal and LOS:

$$\begin{aligned} & \text{If } |r_{ae}(m_i - 1)| > |r_{ae}(m_i + 1)| \\ \varepsilon &= (m_i - 1) + \frac{|r_{ae}(m_i)|}{|r_{ae}(m_i - 1)| + |r_{ae}(m_i)|} \text{ samp} - \text{signal} \end{aligned} \quad (15.15)$$

$$\begin{aligned} & \text{If } |r_{ae}(m_i - 1)| < |r_{ae}(m_i + 1)| \\ \varepsilon &= (m_i) + \frac{|r_{ae}(m_i)|}{|r_{ae}(m_i - 1)| + |r_{ae}(m_i)|} \text{ samp} - \text{signal} \end{aligned} \quad (15.16)$$

Fig. 15.4 Hardware simulator data CIR estimated diagram



Here, r_{ae} the channel impulse response average random time; m_i show the corresponds indicator with code signal.

15.6 Simulation Result

In this paper, author verify the performance of algorithms using the GSS7700 simulator for several simulations. The RF signal from simulator via Low-noise Amplifier to Signal acquisition unit that sampling signal in 25 MHz. The estimated channel impulse response for the GSS7700 hardware simulator is depicted in Fig. 15.4. In this figure, the path attenuation factors can be optional selected from a range of 0–6 dB. It can be known that the estimated channel parameters by the improved POCS is consistent with the reality.

Fig. 15.5 Code phase estimation errors in different algorithms

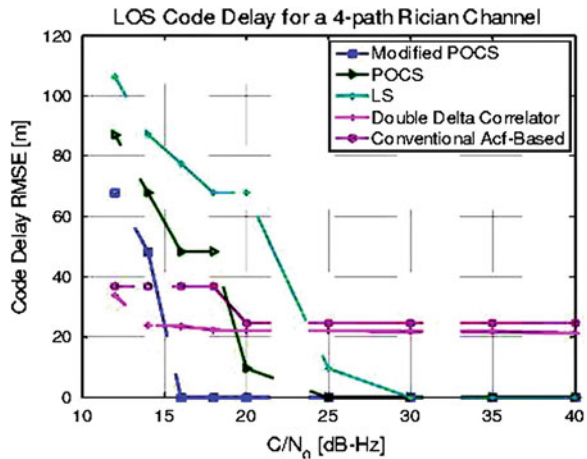
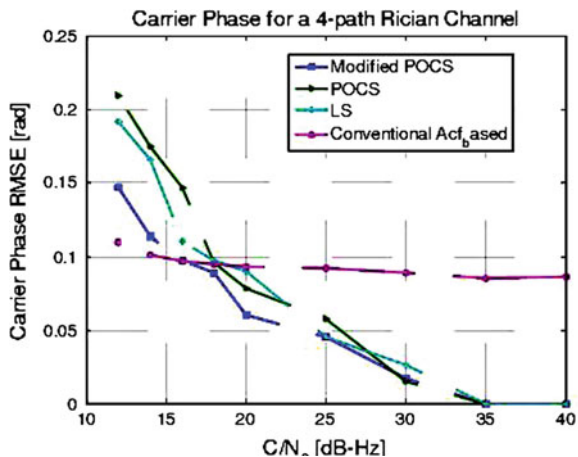


Fig. 15.6 Carrier phase estimation errors in different algorithms



In Figs. 15.5 and 15.6, properties of some different estimation is showed in the 4-path channel allocation. The correlators space 0.07 chip triangle each other.

It is observed from these figures that at low values of C/N₀ (<20 dB), the improved POCS algorithm perform much better than the conventional POCS estimator. In the case of this simulation, the maximum magnitude of the auto-correlation function was close to the true LOS.

15.7 Conclusions

In this paper, author introduce a improved POCS algorithm for code and carrier phase delay estimation. It can be known apparently that the improved POCS algorithm outperforms the conventional POCS at low SNR from the figure. The simulation results illustrate that compared to the conventional error-eliminate techniques, the improved POCS algorithm can decreases the error in the position-fixed obviously also.

References

1. Pahlavan K, Krishnamurthy P (1998) Wideband radio propagation modeling for indoor geolocation applications. *IEEE Commun Mag* 36:60–65
2. Dragunas K (2010) Indoor multipath mitigation. *International Conference on Indoor Positioning and Indoor Navigation, IPIN 2010*, IEEE Press, Zürich, pp 578–584, 15–17 Sep 2010
3. Kostic Z, Pavlovic G (1993) Resolving subchip spaced multipath components in CDMA communication systems. *Vehicular Technology Conference, 1993 IEEE 43rd*, May, pp 469–472
4. Yang C, Porter A (2005) Frequency-domain characterization of GPS multipath for estimation thand mitigation. *ION GNSS 18 International Technical Meeting of the Satellite Division*, Long, Beach, California, pp 2104–2118, Sep 13–16 2005